

**METEOROID, AND DEBRIS SPECIAL INVESTIGATION GROUP PRELIMINARY RESULTS: SIZE-FREQUENCY DISTRIBUTION AND SPATIAL DENSITY OF LARGE IMPACT FEATURES ON LDEF**

**Thomas H. See**

Lockheed Engineering & Sciences Co.  
Houston, Texas 77058  
(713) 483-5027 / FAX (713) 483-5347

**Friedrich Hörz**

NASA Johnson Space Center  
Houston, Texas 77058  
(713) 483-5042 / FAX (713) 483-5347

**Michael E. Zolensky**

NASA Johnson Space Center  
Houston, Texas 77058  
(713) 483-5128 / (713) 483-5347

**Martha K. Allbrooks**

POD Associates, Inc.  
Albuquerque, New Mexico 87106  
(505) 243-2287 / FAX (505) 243-4677

**Dale R. Atkinson**

POD Associates, Inc.  
Albuquerque, New Mexico 87106  
(505) 243-2287 / FAX (505) 243-4677

**Charles G. Simon**

Inst. for Space Sciences & Technology  
Gainesville, Florida 32609  
(904) 371-4778 / FAX (904) 372-5043

**SUMMARY**

The Micrometeoroid and Debris Special Investigation group has documented all craters  $\geq 500 \mu\text{m}$  and penetration holes  $\geq 300 \mu\text{m}$  in diameter on the entire LDEF spacecraft. This report summarizes the observations on the LDEF frame, which exposed aluminum 6061-T6 in 26 specific directions relative to LDEF's velocity vector. In addition, the opportunity arose to characterize the penetration holes in the A0178 thermal blankets, which pointed in nine directions. For each of the 26 directions, LDEF provided time-area products that approach those afforded by all previous space-retrieved materials combined. The objective of this report is to provide a factual database pertaining to the largest collisional events on the entire LDEF spacecraft with a minimum of interpretation. This database may serve to encourage and guide more interpretative efforts and modelling attempts.

The LDEF observations are in qualitative agreement with the salient features of existing models regarding the hypervelocity environment in low-Earth orbit. The crater production rate varies between the forward- and rearward-facing surfaces by more than a factor of 10, possibly by as much as a factor of 20. Within statistical error there is no evidence for differences in the mass-frequency distribution of impactors impinging from diverse radiants.

A complete understanding of LDEF's impact record requires additional documentation of smaller impact features, combined with refined modelling of the dynamic properties of both natural and man-made particles in low-Earth orbit, as well as improvement of crater-scaling relationships and of thin-film penetrations.

**INTRODUCTION**

The Long Duration Exposure Facility (LDEF) exposed a total surface area of approximately  $130 \text{ m}^2$  in low-Earth orbit (LEO) for approximately 5.7 years. This corresponds to an area-time product of approximately  $750 \text{ m}^2$  exposed for a single year, which is almost two orders of magnitude larger than all previous opportunities combined to investigate the hypervelocity particle environment in LEO on space-exposed surfaces. The latter include diverse surfaces exposed on Apollo and Skylab (refs. 1, 2) and on Shuttle (ref. 3), all of time-area products  $< 1 \text{ m}^2/\text{y}$ . Prior to LDEF, the most significant opportunities were in the form of thermal blankets and thin aluminum membranes that possessed a total time-area product of some  $12 \text{ m}^2/\text{y}$  (ref. 4) that were retrieved during the repair of the Solar Maximum Mission spacecraft. These Solar Max surfaces substantiated the presence of a significant man-made debris population in LEO (ref. 5) that combines with the natural particles, largely derived from comets and asteroids, to form a substantial collisional threat to spacecraft in LEO (ref. 6).

Because the number of collisional events is -- to first order -- a linear function of this time-area product, the opportunity offered by LDEF to characterize the natural and man-made particle populations is unique. In addition, there is little prospect of duplicating LDEF's impact record from any space-exposed hardware for at least a decade, much less an opportunity to surpass and improve upon it during a period when spacecraft designers must address collisional hazards to large-scale, long-duration structures in LEO (*i.e.*, Space Station *Freedom*). Analysis of LDEF's

impact record constitutes an observational baseline that will be crucial to the design of future Earth-orbiting flight-systems.

This significance was clearly recognized prior to LDEF's retrieval, and is the primary reason for the establishment of the Meteoroid and Debris Special Investigation Group (M&D SIG). Members of this group resided at the Kennedy Space Center (KSC) throughout the period of LDEF deintegration to document and preserve, for more detailed analysis, the impact record of the entire LDEF spacecraft. While all exposed surfaces were scanned and documented via a set of consistent criteria and procedures, emphasis was placed on those surfaces that were not initially intended to be investigated for impact features. These surfaces were perceived as valuable "targets of opportunity" that would be highly complementary to dedicated micrometeoroid and debris experiments provided by six Principal Investigator (PI) teams. The activities of the KSC M&D SIG team are outlined in (ref. 7), and described in detail in an extensive (600 pages) report (ref. 8).

The following extracts liberally from these reports and is intended to present an overview of the larger impact features on selected surfaces that were not part of dedicated PI-experiments, and that characterize the relative production rates of impact features on the entire spacecraft. Recent theoretical insights (see below) suggest that important dynamic properties, such as the absolute flux and mean impact-velocity of natural and man-made particles in LEO, may be extracted from impacted surfaces that point into specific directions on a non-spinning spacecraft, such as LDEF. As many future structures, including Space Station *Freedom*, will also have fixed attitudes relative to their orbital velocity vector, correct and realistic dynamic modelling becomes crucial for their protection against collisional, and possibly catastrophic damage. LDEF represents a unique and very timely opportunity to test, and hopefully improve on existing models.

The data presented here is limited to factual measurements of crater- and penetration-hole diameters and their frequency of occurrence. These data permit, yet also firmly constrain, more model-dependent, interpretative efforts. Such efforts will focus on the conversion of crater and penetration-hole sizes to projectile diameters (and masses), on absolute particle fluxes, and on the distribution of particle-encounter velocities. These are complex issues (refs. 6, 9, 10, 11, 12, 13, \* ) that presently cannot be pursued without making various assumptions. These assumptions relate, in part, to crater-scaling relationships, and to assumed trajectories of natural and man-made particle populations in LEO, that control the initial impact conditions.

#### RATIONALE FOR THE SELECTION OF ANALYZED SURFACES

The bombardment effects of a non-spinning platform encountering an (assumed) isotropic cloud of hypervelocity particles in LEO are akin to raindrops hitting the windshield of a moving vehicle. More particles are encountered in the forward-facing direction than in the rearward-facing direction, while the velocity distribution of the impactors varies from "fast" in the forward-facing (leading-edge) direction, to "slow" in the opposing (trailing-edge) direction, because particle and spacecraft velocities are added vectorially.

Figure 1 depicts the effective fluxes and mean velocities of natural particles  $>10 \mu\text{m}$  in size that encounter flat, vertical surfaces of specific orientations relative to LDEF's velocity vector. The detailed assumptions and algorithms used by Peterson\* to derive this figure are essentially those of Zook (ref. 9, 10). These model predictions may be tested by a wide variety of LDEF surfaces. Indeed, first order comparisons were offered during the First LDEF

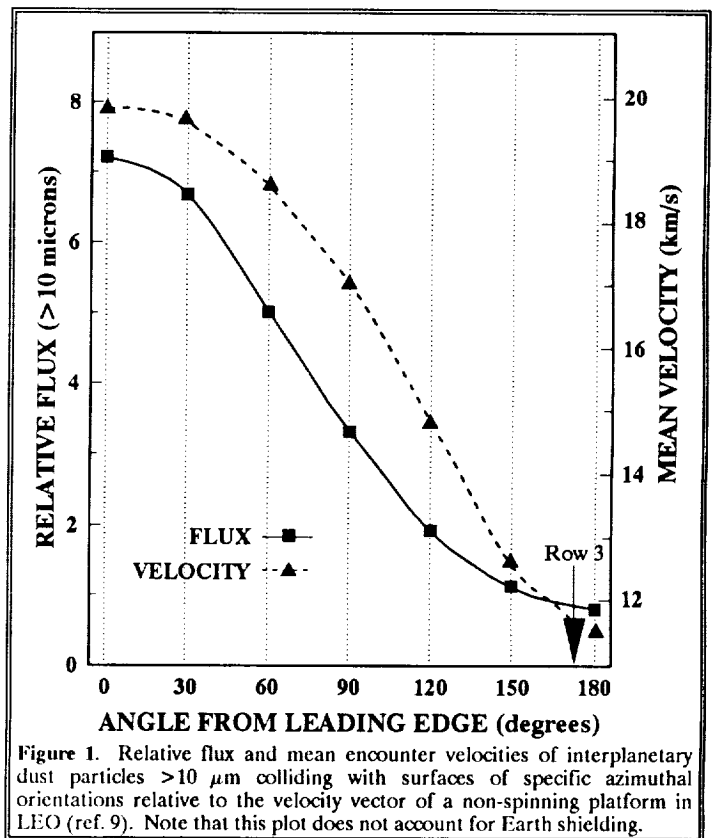


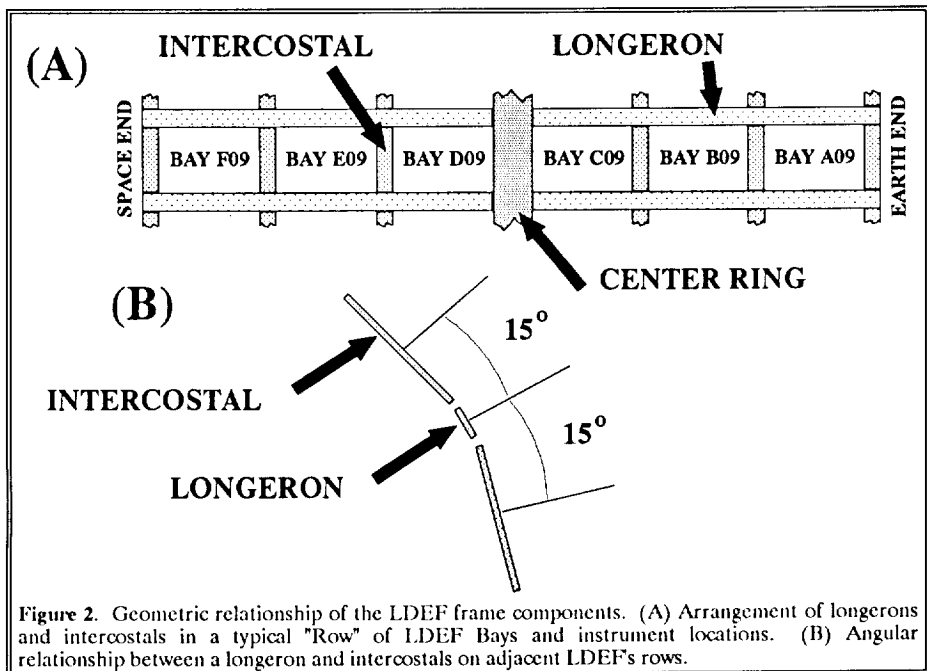
Figure 1. Relative flux and mean encounter velocities of interplanetary dust particles  $>10 \mu\text{m}$  colliding with surfaces of specific azimuthal orientations relative to the velocity vector of a non-spinning platform in LEO (ref. 9). Note that this plot does not account for Earth shielding.

\* Peterson, R.B. (1989) Instrument Pointing Considerations; Report to Cosmic Dust Collection Facility Open Forum, Lunar and Planetary Science Institute, March 1989; unpublished.

Symposium by some dust investigators. In addition, the active Interplanetary Dust Experiment (IDE; ref. 10) will play a substantial role in our understanding of particle dynamics in LEO. While refined calculations and observations may well lead to modifications of Figure 1, the first order findings will remain valid. From Figure 1 it can be seen that the mean encounter velocities range from approximately 20 to 11 km/s for surfaces that point into the leading- and trailing-edge directions, respectively, and that the effective fluxes, at constant projectile size, between those orientations may differ by a factor of 10. Because most impact damage is proportional to the impactor's kinetic energy, the combination of flux and mean velocities results in factors of 30 to 40 difference in the energy flux between leading- and trailing-edge directions, a substantial difference for the design and operation of flight systems. It is obvious that forward-facing systems will sustain more damage than rearward-facing surfaces per unit time, and therefore, that collisional shielding requirements may vary dramatically with specific pointing direction relative to a spacecraft's velocity vector.

The size of any crater or penetration hole depends on a number of physical properties of both the target and projectile material, and on the projectile's mass and impact velocity. A given unit impactor will generate craters of different sizes on LDEF, depending on the instrument location, because of the different effective (mean) encounter velocities as portrayed in Figure 1. The quantitative relationships among these parameters are known for a few LDEF materials, but only over a restricted range and set of initial conditions. Specifically, the prevalent impact velocities in LEO are beyond current laboratory capabilities for most impactors  $> 10 \mu\text{m}$  in diameter. Therefore, it is prudent, if not mandatory, to characterize impact features on identical target materials so that the physical properties of the target can be accounted for or that they reduce to some systematic constant; this permits relative comparisons among surfaces pointing into different directions.

To fully exploit LDEF's potential in contributing to dynamic issues of the particle environment it becomes necessary to study surfaces that are manufactured from identical materials and that are widely distributed over the entire spacecraft. The highly stochastic nature of the collisional environment further mandates that such surfaces be of sufficient surface area to have accumulated a representative population of impact features. Such considerations identify LDEF's aluminum structural frame and the A0178 Teflon thermal blankets as the most outstanding opportunities to learn about the LEO particle populations (in addition to those afforded by dedicated and well calibrated micrometeoroid and debris experiments).



The structural frame of LDEF was manufactured from 6061-T6 aluminum beams that formed an open-grid, 12-sided frame that produced individual instrument bays (Bays A-F) and provided attachment points for the instrument trays; Figure 2 illustrates the pertinent geometric relationships. The longitudinal frame members (-4.6 m long) were termed "longerons", while cross members between longerons were called "intercostals" (-1 m in length). The angle between adjacent instrument rows, defined by the intercostals, was  $30^\circ$  (12-sided cylinder), while the angle between adjoining intercostals and longerons was  $15^\circ$  so that one longeron could accommodate instruments from two adjacent

rows. Individual rows were assigned sequential numbers (1-12), with Row 9 facing in the nominal velocity vector (leading-edge direction) and Row 3 in the trailing-edge direction. For simplicity we assigned the longerons half-row numbers (e.g., longeron 2.5 would reside between Rows 2 and 3). The frame components of the Earth- and space-facing ends (i.e., Bays G & H) of the LDEF spacecraft were essentially flat.

LDEF's structural members represented a total exposed surface area of approximately 15.4 m<sup>2</sup>. The exposed portions of the six intercostals and the center ring had a surface area of approximately 0.61 m<sup>2</sup> per row (1-12), while the longerons (1.5-12.5) exposed approximately 0.54 m<sup>2</sup> in each direction; the Earth- and space-facing ends exposed approximately 0.79m<sup>2</sup> of surface area each. Thus, LDEF's structural members represent impact "detectors" of a single material type pointing in 26 well-defined directions, each possessing  $\geq 0.5$  m<sup>2</sup> of surface area and representing an area-time product  $>3$  m<sup>2</sup>/y. The frame provides an unprecedented opportunity to study impact craters in infinite halfspace targets, and is of extra significance in that the impact behavior of 6061-T6 aluminum, being a common structural material in spacecraft, is fairly well understood (e.g., ref. 10, \* ).

Although not exposed in all 26 directions, identical thermal blankets (i.e., Scheldahl G411500) associated with the sixteen A0178 experiment trays and the one P0004/P0006 experiment tray provided another material type that was widely distributed around the circumference of the spacecraft (i.e., all rows except 3, 9 and 12 contained at least one of these blankets). Each individual blanket exposed approximately 1.2 m<sup>2</sup> of surface area. The time-area product afforded by these thermal blankets was a minimum of 7 m<sup>2</sup>/y in each of these nine LDEF orientations.

The thermal blankets consisted of an outer layer of FEP Teflon (125  $\mu$ m thick) backed by a layer of silver-inconel (200 to 300  $\text{Å}$  thick), which in turn was backed by DC1200 primer and Chemglaze Z306 black conductive paint (80 to 100  $\mu$ m thick), resulting in a total blanket thickness of approximately 180  $\mu$ m. Presently, the impact/penetration behavior of this composite foil is poorly understood; dedicated calibration experiments designed to address such behavior must be conducted. Furthermore, such experiments will contribute to understanding the unusual morphologies of the penetration holes observed in the LDEF blankets (i.e., concentric rings of highly variable geometries, etc., ref. 8). Such features are thought to reflect some form of shock-induced delamination at the interface of the silver-inconel and Teflon layers.

#### FEATURE DESCRIPTIONS AND MEASUREMENTS

Figure 3 illustrates the morphology and associated diameter measurement for typical impact features encountered on the two materials discussed here. Crater diameters refer to rim-crest-to-rim-crest dimensions ( $D_r$ ; Figures 3a & b) and not to the diameter measured at the intercept of the crater walls and the original target surface ( $D_c$ ), which is approximately 25% smaller (refs. 12, 13) than  $D_r$ .

The measurement of the penetration-hole diameter ( $D_h$ ) also refers to a rim-to-rim measurement (Figures 3c & d). Multiple diameter measurements, especially for the case of non-symmetrical holes, were performed and averaged to obtain  $D_h$  for any specific event (ref. 8). The physical penetration hole is modestly smaller than the quoted  $D_h$ ; while no systematic measurements exist, the latter diameter is estimated to differ by  $<10\%$  from  $D_h$  (ref 14). See *et al.* (ref. 8) described the exterior morphologies of these penetration holes which were typically characterized by various colored ring-like, delamination features of variable widths, crispness, spacings, scaled diameters and absolute ring numbers. However, not all penetration holes in these blankets were surrounded by the halo or ring features, and their presence seems to be unrelated to any macroscopic factor or characteristic, such as the diameter of the penetration hole ( $D_h$ ).

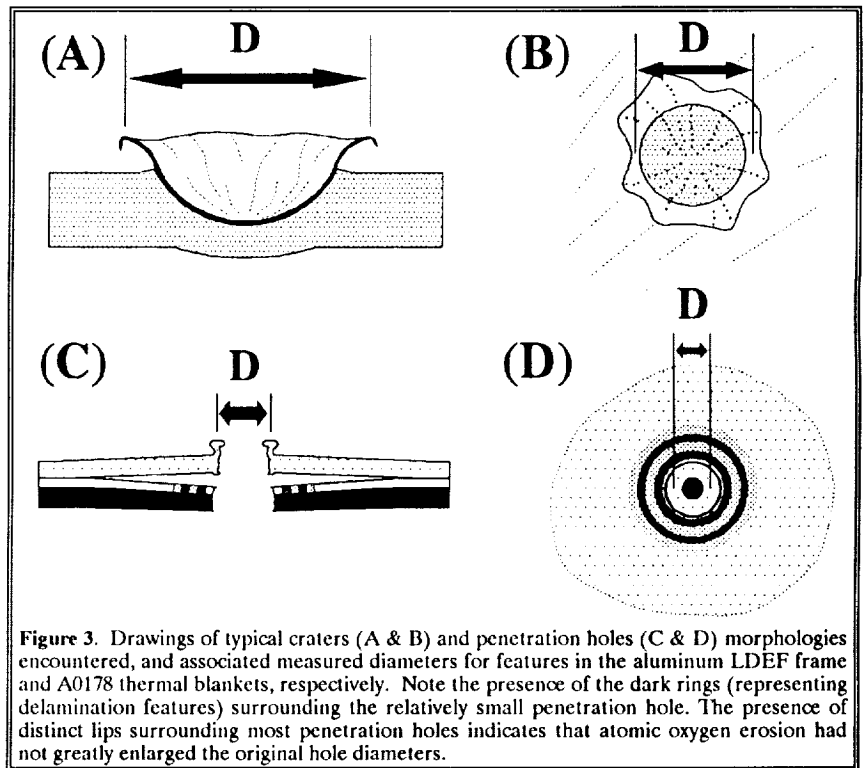


Figure 3. Drawings of typical craters (A & B) and penetration holes (C & D) morphologies encountered, and associated measured diameters for features in the aluminum LDEF frame and A0178 thermal blankets, respectively. Note the presence of the dark rings (representing delamination features) surrounding the relatively small penetration hole. The presence of distinct lips surrounding most penetration holes indicates that atomic oxygen erosion had not greatly enlarged the original hole diameters.

\* Peterson, R.B. (1989) Instrument Pointing Considerations; Report to Cosmic Dust Collection Facility Open Forum, Lunar and Planetary Science Institute, March 1989; unpublished.

During the earliest M&D SIG activities at KSC an operational decision had to be made regarding the cut-off diameter of individual craters and penetration holes to be measured and documented in detail, the latter including location information (with millimeter precision) and stereo photography.

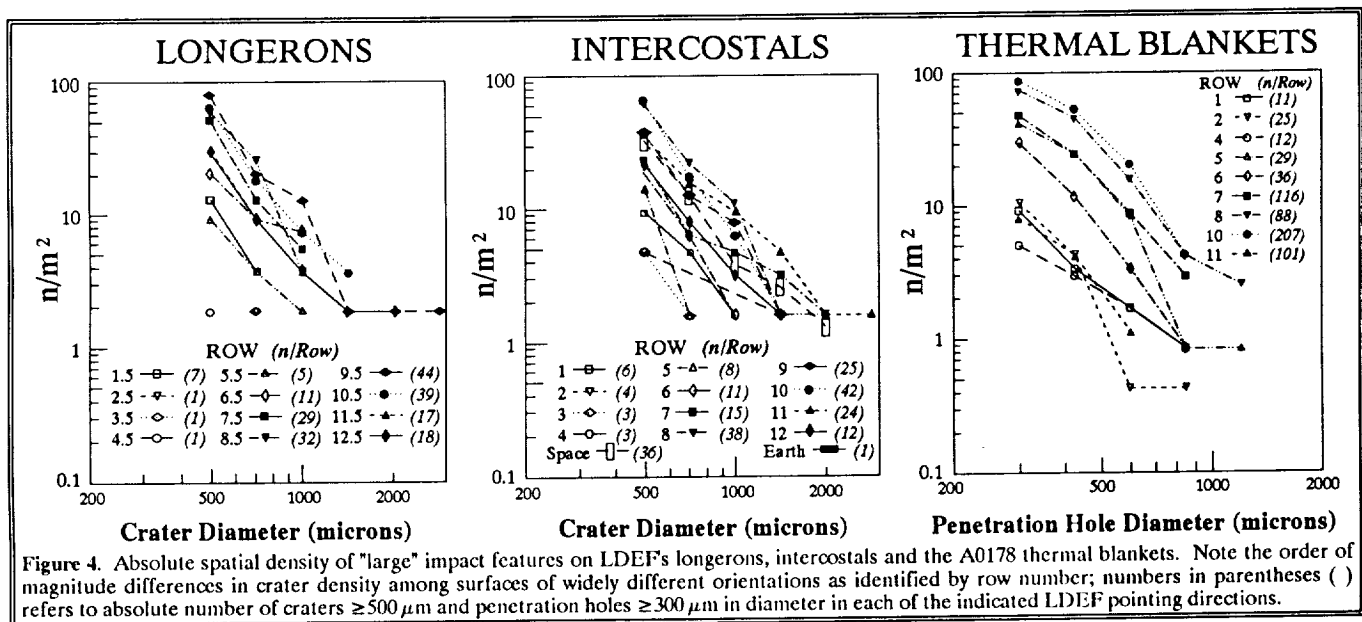
**Table 1.** Distribution of impact features on LDEF. The values listed do not represent a complete count of the number of impact features on LDEF because (1) many surfaces were examined but the exact locations of the <0.3 mm and/or <0.5 mm diameter features were not recorded (*i.e.*, whether they resided on the experimental surfaces or the tray flanges) and (2) during the first several days of M&D SIG documentation activities, only those features that were photodocumented were counted. Thus, the number of features listed in the various categories represent only those features known to exist on that particular surface type, while the "Totals" column depicts the total number of known impacts counted in the various size categories, regardless of their locations.

	CLAMPS, BOLTS & SHIMS	TRAY FLANGES	EXPERIMENTAL SURFACES	LDEF FRAME	THERMAL BLANKETS	TOTALS
<0.3 mm			158		*2831	3069
≥0.3 mm			172		+625	797
<0.5 mm	1318	1923	14171	5171		27385
≥0.5 mm	161	419	2106	432		3118
<b>TOTALS</b>	<b>1479</b>	<b>2342</b>	<b>16687</b>	<b>5603</b>	<b>3456</b>	<b>34336</b>

\* - Count is incomplete; the <0.3 mm diameter features were not counted on F02, C05, C06 and D07  
+ - Count is incomplete; the ≥0.3 mm diameter features from F02 not included.

Obviously, this decision was affected by the maximum workload that could be sustained by the available resources, both observers and equipment, and the ease with which impact features could be observed on various surface materials. Cut-off diameters of 500 μm for craters in infinite halfspace targets, and 300 μm for penetration holes in thermal blankets were chosen. This dual size threshold was employed due to the differing processes associated with hypervelocity impacts into foils versus materials of much greater thickness. These cut-off diameters were applied rigorously and systematically to all LDEF surfaces, including the longerons and intercostals of LDEF's frame, leading to a complete inventory of all craters ≥500 μm in diameter for the entire spacecraft. In addition, the total number of impact structures between these cut-off diameters and approximately 50 μm in diameter, as observed with the naked eye, was counted and recorded as a single, cumulative number. However, the latter is particularly operator-sensitive, and dedicated studies are needed to characterize features smaller than the (large) cut-off diameters. As detailed in Table 1, these procedures yielded approximately 35,000 impacts ≥50 μm in diameter, which must constitute a minimum value, and approximately 4,000 larger structures that were documented individually and that represent a quantitative account of LDEF's "large" impact features.

This report summarizes these large events exclusively. The impact craters contained on LDEF's frame comprise a set of 432 individually documented craters, while the thermal-blanket data are based on 625 penetrations. These represent about 10% and 78%, respectively, of all large craters penetrations on the entire spacecraft.



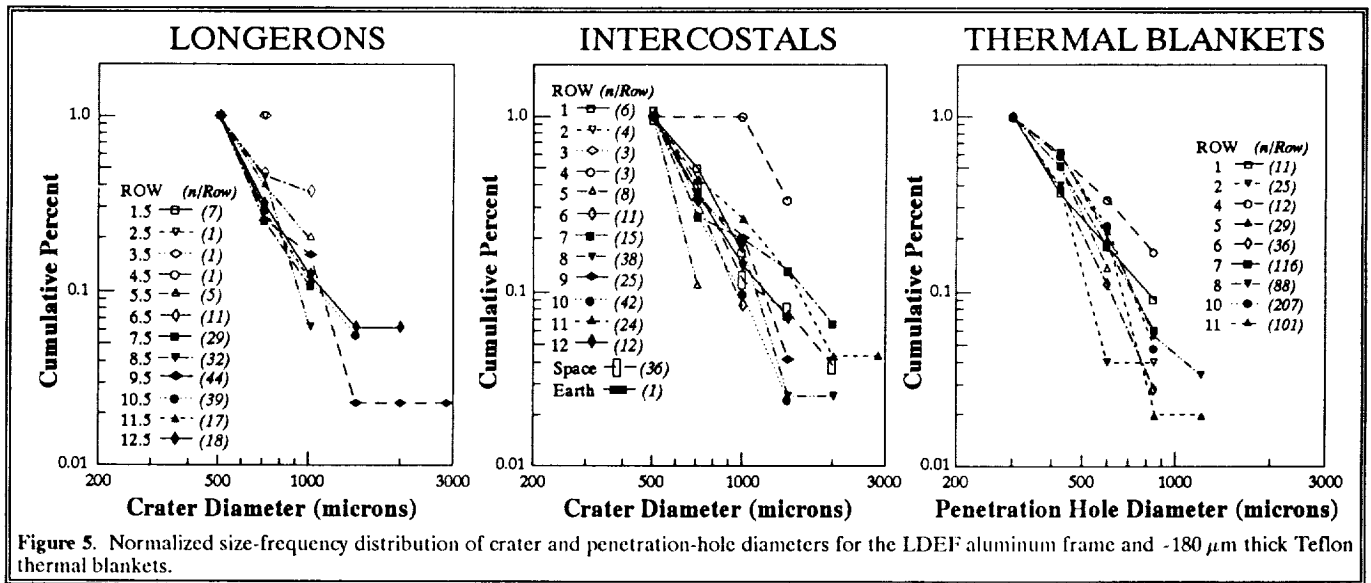


Figure 5. Normalized size-frequency distribution of crater and penetration-hole diameters for the LDEF aluminum frame and -180  $\mu\text{m}$  thick Teflon thermal blankets.

## RESULTS

The cumulative size-frequency distributions and spatial densities of large craters and penetration holes are illustrated in Figure 4 where they are grouped into specific viewing directions, identified by LDEF row. Unfortunately, even for such substantial time-area products, the total number of events is still generally small, leading to poor statistics and large scatter in the data. We calculated two-sigma (95% confidence level) error bars (not illustrated for the sake of clarity in Figure 4) and conclude that effective crater-production rates depend on instrument orientation and that relative size-frequency distributions could be identical.

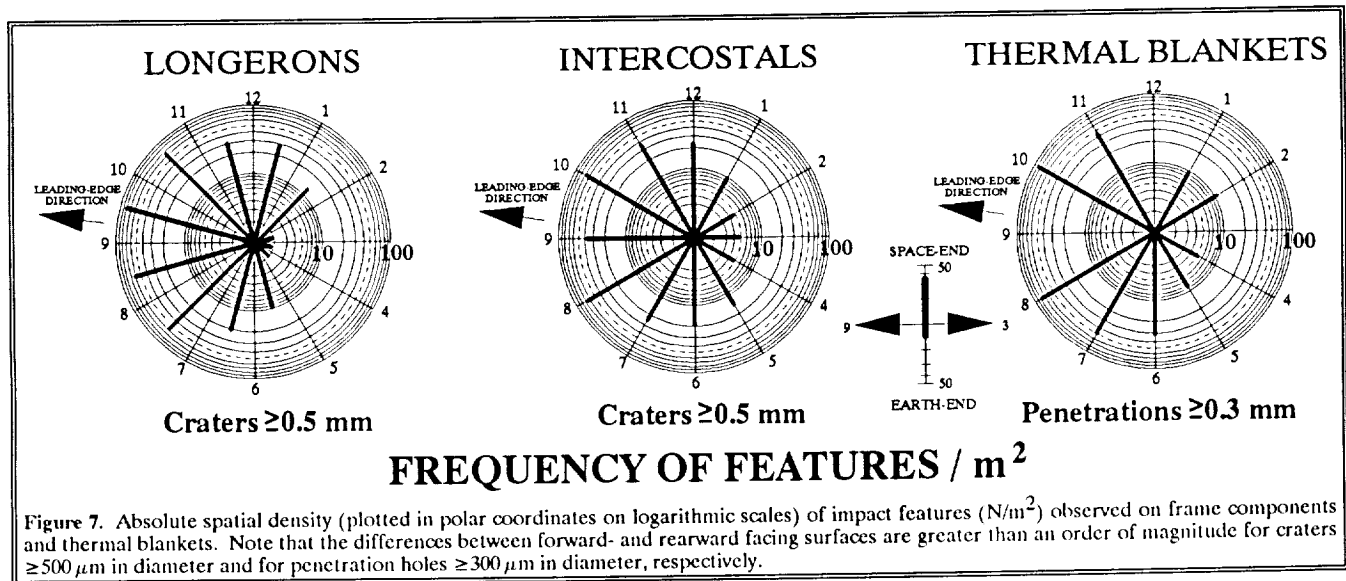
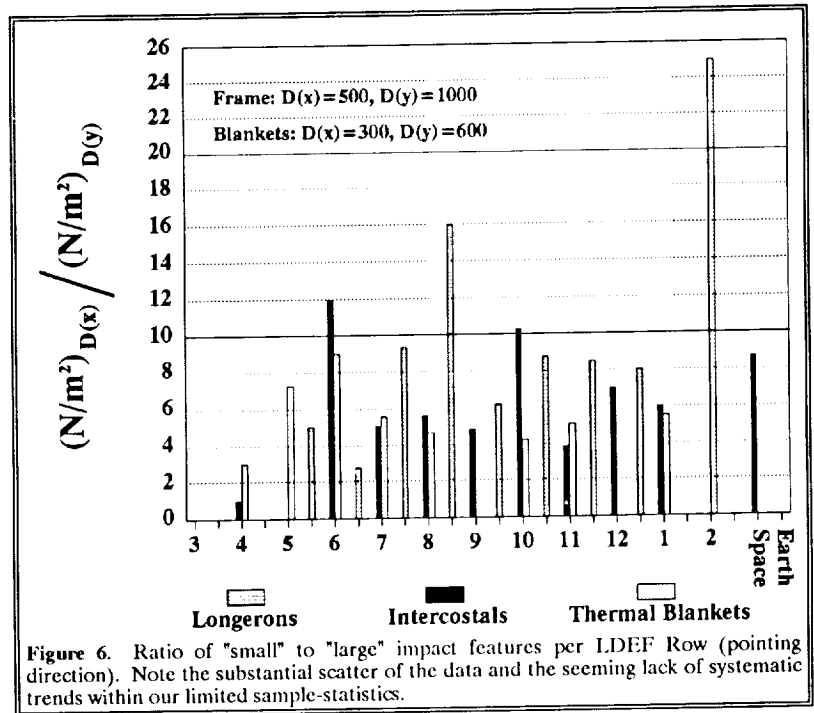
If taken literally, substantial variations in relative mass-frequency of the impactor populations would be obtained from the normalized crater- and penetration frequency data illustrated in Figure 5. Clearly, the latter are heavily affected by the presence or absence of a few, large, stochastic events, and is the reason why detailed measurements of (distribution) slope and associated implications are unwarranted. Nevertheless, Figure 6 illustrates the statistically most meaningful (yet tentative) ratios of small to large events that may be extracted from the data sets. "Small" refers to the (somewhat arbitrary) cut-off limits of (*i.e.*,  $D_r = 500 \mu\text{m}$  and  $D_h = 300 \mu\text{m}$ ), while "large" refers to events twice that size (*i.e.*,  $D_r = 1000$  and  $D_h = 600 \mu\text{m}$ ). The latter size features were present on all surfaces, but total numbers are generally small. Figure 6 exhibits no systematic trends that may be related to instrument pointing direction. Note that the thermal blankets exhibit relatively high frequencies for large events on the forward-facing directions, while the longeron data seem to indicate the opposite. Obviously, both trends cannot be correct simultaneously and we conclude from Figures 4, 5 and 6 that the statistics for features larger than our threshold diameters may not suffice to state, with confidence, whether or not the size frequency of projectiles varies with viewing direction. Additional data are needed on small-scale features to provide firm answers to such questions.

Figure 7 displays the absolute frequency of observed features as a function of instrument orientation in an LDEF specific reference frame. We are aware that the actual leading edge was approximately  $8^\circ (\pm 0.4^\circ)$  off, toward Row 10, from the nominally planned Row 9 direction (ref. 14). This off-set, however, does not invalidate the premission-assignment of Row 9 as the "leading-edge", and of Row 3 as the "trailing-edge", an assignment that we maintained throughout this report. Figure 7 illustrates, in polar coordinates on logarithmic scales, the observed, absolute crater density ( $\text{N}/\text{m}^2$ ) for craters  $\geq 500 \mu\text{m}$  in diameter on the longerons and intercostals, as well as the number of penetration holes  $\geq 300 \mu\text{m}$  in diameter for the thermal blankets. For clarity and ease of comparison, Figure 8 illustrates the data in histogram form, both in absolute and relative terms, the latter after normalization to the maximum spatial densities observed on the Row 10 intercostals (crater density) and thermal blankets (penetration-hole density).

It seems apparent that there is a strong dependence on pointing direction as implied by Figure 1, and -- in a gross sense -- the observations are consistent with modelled expectations. The effective production rate of craters or penetration holes of constant size seems to differ by more than a factor of 10 between the highest and lowest frequencies.

Unfortunately, leading- and trailing-edge crater densities accessible to the M&D SIG are confined to the intercostals only; no thermal blankets occupied LDEF Rows 3 and 9, and the longerons were 15° off-set from each row. Somewhat surprisingly, as detailed and emphasized earlier (ref. 15), the Row 9 longeron displays a modest crater population which is distinctly smaller than the adjacent longerons and intercostals. We consider the Row 9 intercostal data to be non-representative. Adjacent intercostals on Rows 8 and 10, and longerons at locations 8.5 and 9.5 have consistently higher crater densities. Because of the orbital precession of the Earth (-8°/day), any anisotropy in particle flux would be substantially and rapidly smeared out over neighboring LDEF

locations; it seems implausible from a dynamic point of view to sustain the low impact rates implied by the Row 9 intercostals and at the same time cause the apparent higher rates on adjacent surfaces that are only 15° and 30° apart, respectively. Supporting evidence for this interpretation comes from the general trends displayed by the thermal blankets as well, that also yield maxima in the forward-facing directions (Rows 8 and 10).



In detail, as previously mentioned, LDEF's orbital plane was modestly off-set by approximately 8° in the Row 10 direction. Note that the highest crater densities on LDEF were obtained on the 9.5 longeron, and that the spatial density of penetration holes is highest for Row 10. These trends differ qualitatively from those expected on the basis of Figure 1, which assumes bilateral symmetry about the plane of motion. It appears that LDEF received more impacts from the general direction of Rows 10 and 11 than on the symmetrically equivalent Rows 8 and 9.

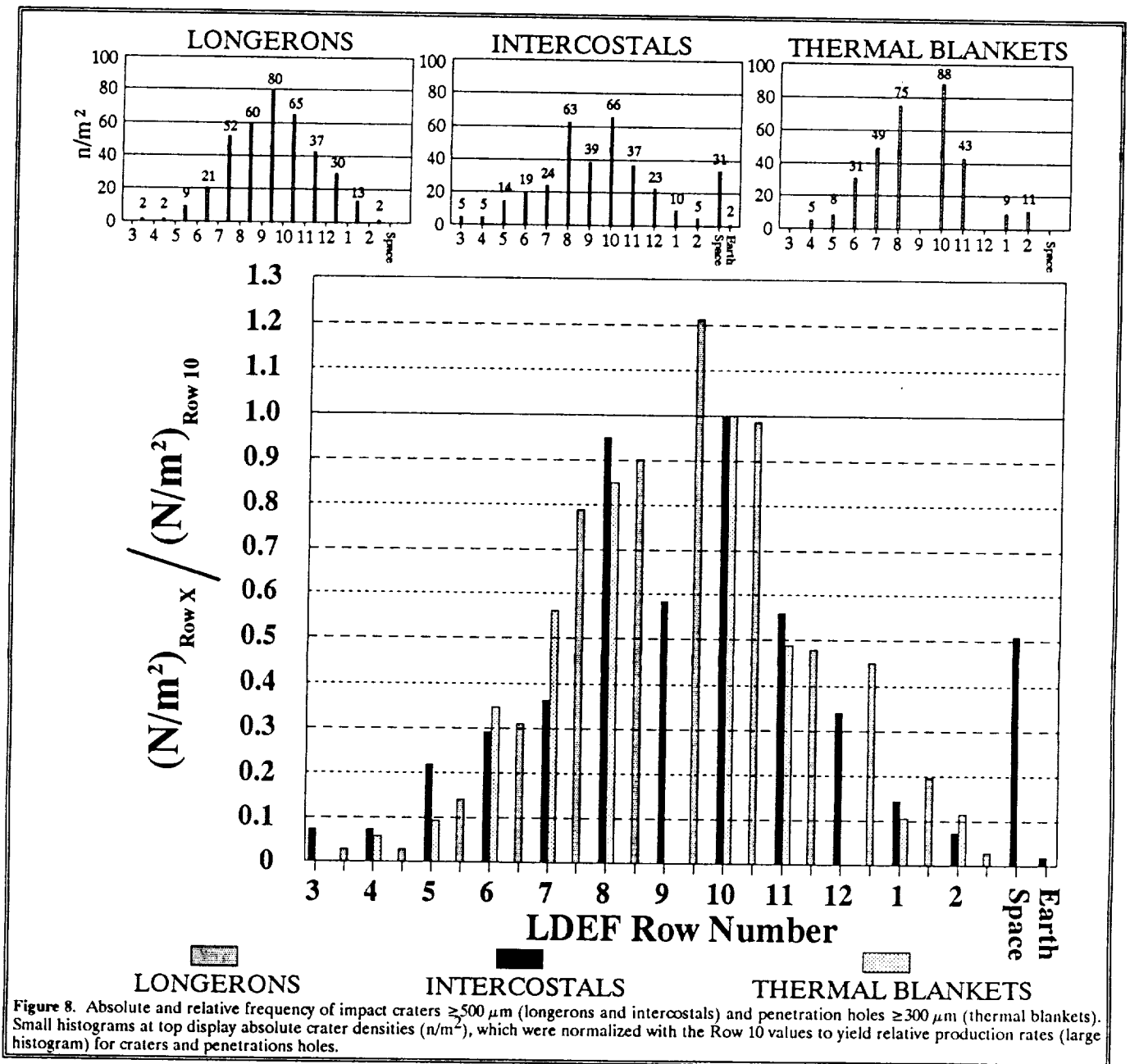


Figure 8. Absolute and relative frequency of impact craters  $\geq 500 \mu\text{m}$  (longerons and intercostals) and penetration holes  $\geq 300 \mu\text{m}$  (thermal blankets). Small histograms at top display absolute crater densities ( $n/m^2$ ), which were normalized with the Row 10 values to yield relative production rates (large histogram) for craters and penetrations holes.

If the observed minima and maxima of crater and penetration-hole densities were taken literally, the difference in calculated production rates for impact features (at constant size) between trailing- and leading-edges would be about 1:43 (longerons), 1:14 (intercostals), and 1:17 (thermal blankets). Using a more reasonable and statistically improved approach (*i.e.*, averaging rearward-facing Rows 2, 3 and 4 and forward-facing Rows 8, 9 and 10), results in production rates for impact features between these principle orientations of 15-20 for impact features of identical sizes.

Again, we emphasize the raw observations presented throughout this report will have to be converted to projectile properties, such as mass and (mean) impact velocity, before the above production rates at constant feature diameter may be converted into absolute particle fluxes. Presently, such conversions can be accomplished only by making various assumptions.

## DISCUSSION

The largest surfaces and time-area products ever retrieved from space were scanned for relatively large impact features in a very careful and rigorous manner. While these investigations were performed in parallel with other LDEF deintegration activities at KSC, the quality of the data obtained was not affected by some of the unavoidable constraints applied during these complex operations. The major constraint related to time, which dictated the cut-off diameters for craters ( $\geq 500 \mu\text{m}$ ) and penetration holes ( $\geq 300 \mu\text{m}$ ). It is recognized that more detailed and time-consuming studies are needed to characterize smaller impact features. To this end the M&D SIG acquired representative materials from LDEF that are being curated at JSC, and which are now available for detailed study by qualified investigators.

The current findings are in qualitative agreement with existing model-predictions that suggest highly differential bombardment histories for surfaces pointing into specific directions relative to the velocity vector of a non-spinning platform in LEO. The production rates for craters  $\geq 500 \mu\text{m}$  in diameter in 6061-T6 aluminum and penetration holes  $\geq 300 \mu\text{m}$  in diameter in thin foil materials (Teflon;  $180 \mu\text{m}$  thick) differ by more than a factor of 10, and possibly by as much as a factor of 20 between leading- and trailing-edge facing surfaces. These are substantial differences and must translate into serious engineering considerations during the design of future, large-scale, long-duration platforms in LEO. The crater and penetration-hole counts do represent a valuable, empirical database to guide the design and possible collisional shielding requirements for future spacecraft, most immediately the Space Station *Freedom*. However, substantial additional work is needed in order to understand LDEF's bombardment history and the collisional hazard in LEO.

We recommend that the observable impact record be expanded to include smaller impact features. In addition, future efforts must concentrate on additional theoretical work concerning the interactions of natural and man-made impactors with non-spinning platforms, an effort which inevitably will also result in averaged conditions for spin-stabilized spacecraft. Furthermore, efforts are needed to experimentally determine the penetration behavior of the LDEF thermal blankets and to extrapolate impact conditions beyond current laboratory capabilities by means of suitable scaling-relationships to those conditions prevailing in LEO. Progress in the area of orbital dynamics, as well as crater and penetration mechanics must be combined in a highly iterative fashion to better understand and cope with the collisional environment in LEO. It was the intent of this report to demonstrate how LDEF has already contributed to these efforts, and how it can and may continue to do so.

## REFERENCES

- 1) Cour-Palais, B.G. (1979), Results of the examination of the Skylab/Apollo windows for micrometeoroid impacts, *Proc. Lunar Planet. Sci. Conf. 10<sup>th</sup>*, p. 247-265.
- 2) Clanton, U.S., Zook, H.A. and Schultz, R.A. (1980) Hypervelocity impacts on Skylab IV/Apollo windows, *Proc. Lunar Planet. Sci. Conf. 11<sup>th</sup>*, p. 2261-2273.
- 3) McDonnell, J.A.M., Carey, W.C. and Dixon, D.G. (1984) Cosmic dust collection by the capture cell technique on the Shuttle "Pathfinder" mission, *Nature*, 309, #5965, p. 237-240.
- 4) Warren, J.L. and 10 Co-authors, (1989) The detection and observation of meteoroid and space debris impact features on the Solar Max satellite, *Proc. Lunar Planet. Sci. Conf., 19<sup>th</sup>*, p. 641-657.
- 5) Rietmeijer, F.J.M., Schramm, L., Barrett, R.A., McKay, D.S. and Zook, H.A. (1986) An inadvertent capture cell for orbital debris and micrometeoroids; the Main Electronics Box thermal blanket of the Solar Maximum Satellite, *Adv. Space. Res.*, 6, p. 145-149.
- 6) Kessler, D.J. (1991) Orbital Debris Environment for Spacecraft in low Earth orbit, *J. Spacecraft*, 28, 3, p. 347-351.
- 7) See, T.H., Allbrooks, M.K., Atkinson, D.R., Sapp, C.A., Simon, C.G. and Zolensky, M.E., Meteoroid and Debris Special Investigation Group Data Acquisition Procedures. First LDEF Post-Retrieval Symposium, NASA CP-3134, 1992.

- 8) See, T.H., Allbrooks, M.A., Atkinson, D.R., Simon, C.G. and Zolensky, M. (1990) Meteoroid and Debris Impact Features Documented on the Long Duration Exposure Facility, A Preliminary Report, Publication #84, JSC #24608, 583 pp.
- 9) Zook, H.A. (1987) On cosmic dust trajectory measurements and experiment pointing considerations, in Progress towards a Cosmic Dust Collection facility on Space Station, Mackinnon, I.D. and Carey, W.C., eds., Lunar and Planetary Institute, *LPI Technical Report 88-01*, p. 76-77.
- 10) Zook, H.A. (1991) Meteoroid directionality on LDEF and asteroidal versus cometary sources (abstract). *Lunar Planet. Sci. XXII*, Lunar and Planetary Institute, Houston, Tx., p. 1577-1578.
- 11) Mullholland, J.D. and 8 Co-authors (1991) IDE Spatio-temporal fluxes and high time-resolution studies of multi-impact events and long-lived debris clouds, First LDEF Post-Retrieval Symposium, NASA CP-3134, 1992.
- 12) Cour-Palais, B.G. (1987) Hypervelocity Impacts in Metals, Glass, and Composites, *Int. J. Impact Eng.*, 5, p. 681-692.
- 13) Hörz, F., Messenger, S., Bernhard, R., See, T.H. and Haynes, G. (1991) Penetration phenomena in Teflon and aluminum films using 50-3200  $\mu\text{m}$  glass projectiles (abstracts), *Lunar Planet. Sci. XXII*, Lunar and Planetary Institute, p. 591-592.
- 14) Gregory, J.C. and Peters, P.N. (1991) LDEF attitude measurement using a pinhole camera with a silver/oxygen atom detector, First LDEF Post-Retrieval Symposium, NASA CP- 3134, 1992.
- 15) Zolensky, M., Atkinson, D., See, T.H., Allbrooks, M., Simon, C., Finckenor, and Warren, J. (1991) Meteoroid and Orbital Debris Record of the Long Duration Exposure Facility's Frame, *J. Spacecraft and Rockets*, 28, #2, p. 204-209.